

Original Research

ALYREF associated with immune infiltration is a prognostic biomarker in hepatocellular carcinoma

Zhen-Zhen Wang^{a,1}, Tao Meng^{b,1}, Ming-Ya Yang^{c,1}, Wei Wang^a, Yan Zhang^d, Yu Liu^a, An-Qi Han^a, Jin Wu^a, Hui-xiao Wang^{e,*}, Bo Qian^{d,*}, Li-Xin Zhu^{a,*}

^a Department of General Surgery, Central Laboratory, The First Affiliated Hospital of Anhui Medical University, Hefei 230022, China

^b Department of General Surgery, The First People's Hospital of Hefei, Hefei 230000, China

^c Department of Haematology, The First Affiliated Hospital of Anhui Medical University, Hefei 230022, China

^d Department of General Surgery, The Second Affiliated Hospital of Anhui Medical University, Hefei 230022, China

^e Department of Medicine, The Second People's Hospital of Anhui Province, Hefei 230000, China



ARTICLE INFO

Keywords:
HCC
ALYREF
Prognosis
Immune
Nomogram

ABSTRACT

Background: Although ALYREF has been demonstrated to have a role in a number of malignancies, its role in hepatocellular carcinoma (HCC) has received little attention. Our objective was to research at the prognostic value, biological role and relevance of ALYREF to the immune system in HCC.

Methods: The expression of ALYREF and its relationship with clinical parameters of HCC patients were analyzed by liver cancer cohort (LIHC) of The Cancer Genome Atlas. The expression and prognosis were verified by immunohistochemistry experiments. Gene transfection, CCK-8, scratch healing, transwell invasion and flow cytometry were used to assess the molecular function of ALYREF *in vitro*. The TIMER and TISIDB online data portals were used to assess the relevance of ALYREF to immunization. Stepwise regression analysis of ALYREF-related immune genes in the LIHC training set was used to construct a prognostic risk prediction model. Also, construct a nomogram to predict patient survival. The testing set for internal verification.

Results: Knockdown of ALYREF changed the biological phenotypes of HCC cells, such as proliferation, apoptosis, and invasion. In addition, the expression of ALYREF in HCC affected the level of immune cell infiltration and correlated with the overall survival time of patients. The constructed immune prognostic model allows for a valid assessment of patients.

Conclusion: ALYREF is increased in HCC, has an impact on cellular function and the immune system, and might be used as a prognostic marker.

Introduction

Primary liver cancer is very malignant, and its mortality rate has already risen to third place in 2020. The most common pathological type is hepatocellular carcinoma (HCC), which accounts for 75–85% of cases. [1,2]. Due to the insignificant symptoms in the early stage, many patients were unable to undergo hepatectomy at the time of diagnosis [2]. Immunotherapy has emerged as a promising alternative therapy for advanced HCC in recent years, which has brought opportunities for the patient [3]. However, immunotherapy is not suitable for all HCC patients. Prognostic immune markers can be used to screen patients for this treatment [4]. With the increase of combined immunotherapy regimens,

more effective prognostic immune markers and immunotherapy targets are needed to be further explored [5].

ALYREF, also termed as THOC4, is an adaptor for mRNA export and is involved in nuclear export of mRNA, 3' end processing, and regulation of mRNA and genome stability ([6,7]). ALYREF has been found to be upregulated in a number of malignancies and is connected with poor prognosis, including bladder cancer, glioblastoma, and head and neck squamous cell carcinoma. [8–12]. Xue et al [13] have pointed out that ALYREF might be a prognostic factor for HCC. Nevertheless, the specific biological function of ALYREF in HCC and its relationship to the immune system have not been reported.

It was found in this study, ALYREF is associated with the prognosis of

* Corresponding authors.

E-mail addresses: whx1066@126.com (H.-x. Wang), qianbo79@163.com (B. Qian), zhulixin@ahmu.edu.cn (L.-X. Zhu).

¹ These authors contributed equally to this work.

Table 1
Correlation between *ALYREF* expression level and clinicopathological characteristics in 120 hepatectomy specimens.

Characteristics	n	<i>ALYREF</i>		χ^2	p Value
		Low expression (n=64)	High expression (n=56)		
Age (year)					
≤60	83	43	40	0.252	0.616
>60	37	21	16		
Gender					
Female	20	11	9	0.027	0.870
Male	100	53	47		
Cirrhosis					
No	27	15	12	0.069	0.793
Yes	93	49	44		
HBsAg					
Negative	22	12	10	0.016	0.900
Positive	98	52	46		
Relapse					
No	37	22	15	0.807	0.369
Yes	83	42	41		
BCLC Stage					
Stage 0+Stage A	73	43	30	4.464	0.107
Stage B	17	10	7		
Stage C	30	11	19		
Venous infiltration					
No	90	53	37	4.464	0.035
Yes	30	11	19		
Tumor size (cm)					
≤2	16	13	3	6.805	0.033
2~5	46	20	26		
>5	58	31	27		
AFP (ng/ml)					
<200	72	44	28	4.375	0.036
≥200	48	20	27		
AJCC Stage					
I	72	45	27	6.275	0.043
II	11	5	6		
III	37	14	23		
Histologic Grade					
G1+G2	81	50	31	7.057	0.008
G3+G4	39	14	25		

HCC with The Cancer Genome Atlas (TCGA) analysis. The validations of this study include: [1] immunohistochemistry of HCC sections was used to investigate the link between *ALYREF* expression and patient prognosis; [2] HCC cell lines was adopted to study the biological characteristics of *ALYREF* with gene transfection and knockout methods; [3] the relationship between *ALYREF* expression and immunomodulator genes was systematically assessed through online databases; [4] the prognostic immune model was constructed based on *ALYREF*-related immune genes, which has passed internal validation and can be used to assess the prognosis of HCC patients.

Methods and materials

Public data acquisition and analysis

The liver cancer dataset (LIHC) of the TCGA (<https://portal.gdc.cancer.gov/>) was used to obtain patient clinical information and mRNA expression profiles (RNA-Seq, FPKM format) containing 374 HCC and 50 paraneoplastic tissue samples. RNA-Seq was analyzed using the R package 'limma' to examine the difference in *ALYREF* expression between HCC and normal liver tissues. The R package "ggpubr" for analyzing the correlation between *ALYREF* and clinical parameters, and survival curves were constructed by Kaplan-Meier analysis.

Table 2
Sequences of siRNAs.

Name	Sequence (5'-3')
Negative control siRNA (si#NC)	sense: UUCUCCGAACGUGUCACGUTT, antisense: ACGUGACAGUUCGGAGAATT
<i>ALYREF</i> siRNA1 (si#1)	sense: CCAUGAACAUUCAGCUUGUTT, antisense: ACAAGCUGAAUGUUAUGGTT
<i>ALYREF</i> siRNA2 (si#2)	sense: GAAUUUGGAACGCUGAAGATT, antisense: UCUUCAGCGUCCAAAUUCTT

Gene set enrichment analysis (GSEA)

The median expression of *ALYREF* in LIHC RNA-seq was used as a node to split patients into high and low expression groups. The GSEA software (version 4.1.0) reference molecular signature database (MSigDB) was used to analyze the pathways that *ALYREF*-related genes may be involved in regulation.

Immunohistochemistry

The data and paraffin specimens from 120 patients with HCC who undergone radical hepatectomy in the First Affiliated Hospital of Anhui Medical University during 2011–2015 were harvested. Survival information of patients was obtained through telephone follow-up. The clinical parameter was present in Table 1. Before the hepatectomy, none of the patients had had any other treatment. SP method was used for the immunohistochemical staining: primary antibody (anti-*ALYREF*, 1:200, abcam, UK) was added after tissue section dewaxing, hydration, antigen repair, and blocking nonspecific binding sites. The primary and secondary antibodies were incubated for 1 h at 37 °C and 20 min at room temperature, respectively. Diaminobenzidine (DAB) was used for color development, and the slides were mounted after counterstaining with hematoxylin. There were four categories to record the percentage of positive cells: 1 (0% to 15%), 2 (15% to 50%), 3 (50% to 75%), and 4 (75% to 100%), respectively. According to the staining intensity, they were divided into three categories: 1 (mild), 2 (moderate), and 3 (severe), respectively. The two scores are multiplied to get the final score: low expression group [1–4] and high expression group [6–12]. The objects are classified by pathologists who had no access to clinical data.

Cell culture and transfection

Cell Bank of Chinese Academy of Sciences provided HCC cell lines (Huh7, Hep3B, HepG2, and HCCLM3) as well as hepatocyte cell line HL-7702. DMEM medium with 10% fetal bovine serum was used to cultivate all cells in a cell incubator (5% CO₂, 37 °C). Purchased small interfering RNAs (siRNA; GenePharma, China) were transfected into HCC cell lines Huh7 and Hep3B using lipofectamine 3000 (invitrogen, USA) according to the instructions. After 48 h of cell transfection, the transfection efficiency was checked by real-time fluorescence quantitative PCR (RT-qPCR) and Western Blotting. The siRNA sequences are listed in Table 2.

RNA extraction and RT-qPCR

A reverse transcription kit (TOYOBO, Japan) was used to convert total cellular RNA extracted with TRIzol (Invitrogen, USA) into cDNA. Each sample was analyzed in triplicate by RT-qPCR using SYBR green Master mix (Accurate Biology, China) on an agilent Mx3000p instrument. The gene *GAPDH* was employed as an internal reference with the primer sequences: forward 5'- CCACTCTCCACCTTTG-3'; reverse 5'- CACCACCTGTTGCTGT-3'. *ALYREF* primer sequences: forward 5'- GAAACTGCTGGTGTCCAATC-3'; reverse 5'- CACGTCTGCTGTTCC-TAAGC-3'.

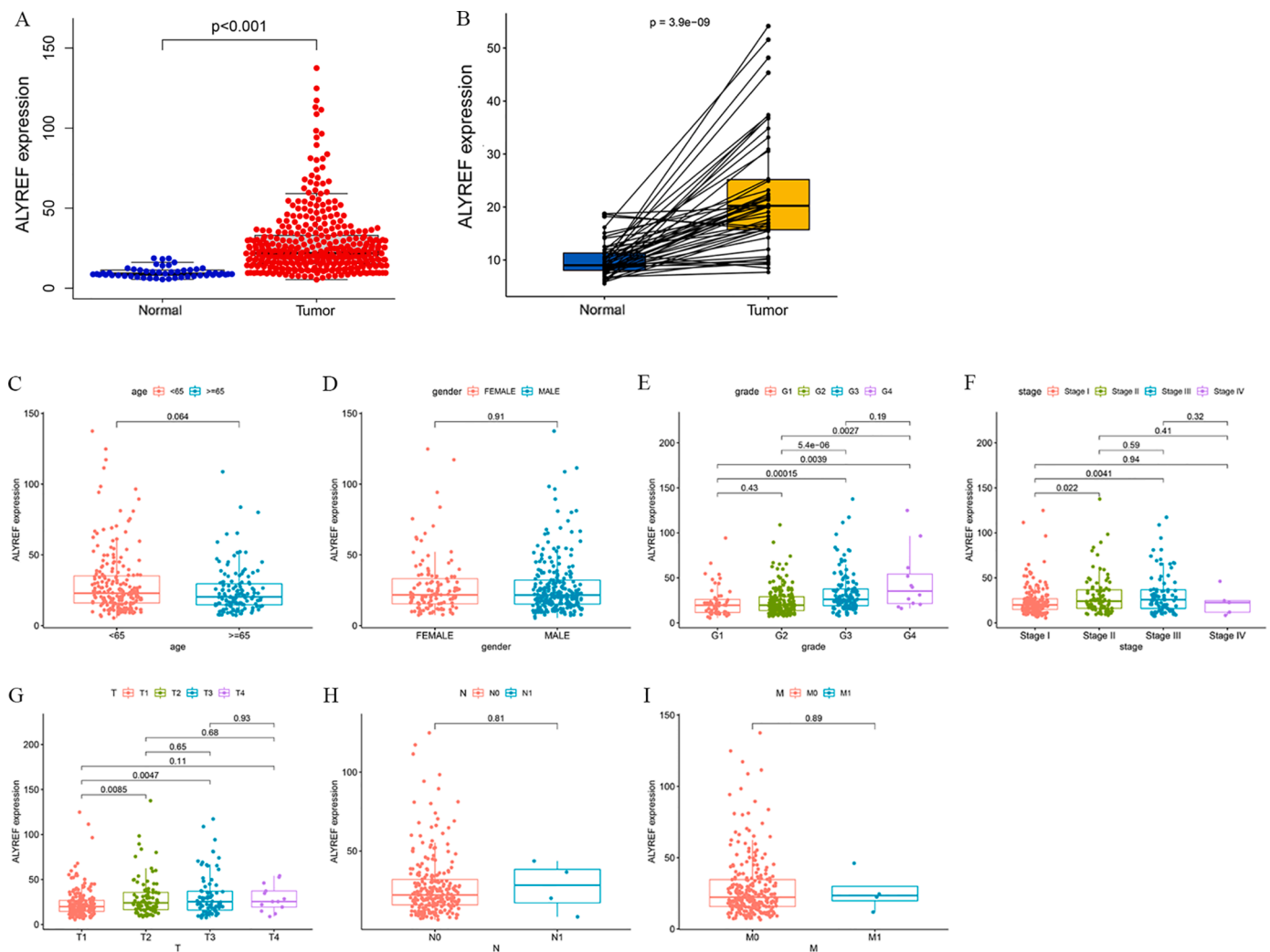


Fig. 1. Expression of *ALYREF* in different subgroups based on the clinical characteristics of TCGA. (A) *ALYREF* expression was increased in HCC compared to normal liver tissue. (B) *ALYREF* expression is higher in HCC than in paired paracancerous tissues. (C–I) Expression levels of *ALYREF* in different clinical trait subgroups.

Cell proliferation assay

Cell Counting Kit-8 (CCK-8, biosharp, China) assays: cells were transfected for 24 h and inoculated into 96-well plates (3×10^3 cell/well) with 100 l complete medium per well. CCK-8 (10 l/well) was added at 0, 22, 46, 70 and 94 h after inoculation, respectively. The absorbance at 450 nm was measured using a microplate reader (BioTek, USA) after 2 h of incubation in the incubator. The experiment was carried out three times, each time with four replicate wells per sample.

Colony formation assay: the cells were transfected for 24 h, inoculated into 6-well plates (1000 cells/well) and cultured for 12 days, washed in PBS, fixed for 30 min with 4% paraformaldehyde, then stained with 0.1% crystal violet for 20 min. The number of cell colonies was calculated by taking pictures after washing.

Scratch healing assay

Cells were inoculated into 6-well plates and transfected when 80% confluency was reached. After the cells formed a monolayer, scratches were made with a 200 l sterile pipette tip, wash out excess cells with PBS, and continue the culture with serum-free DMEM. Photographs were taken under a microscope (Olympus 1 × 51, Japan) after 24 h, and the percentage of wound healing area was subsequently calculated.

Transwell Invasion assay

Chambers with a membrane pore size of 8 μm were covered with Matrigel (Corning, USA) and placed in 24-well plates. The cells were washed in PBS and resuspended in DMEM after being transfected for 24 h. Add 600 l of DMEM containing 20% FBS to the 24-well plate where the chamber is placed, then inoculate 200 l of cell suspension into the chamber (1×10^5 cells/well). After culturing for 48 h, the cells were fixed with 4% paraformaldehyde for 30 min, dried and stained with 0.1% crystal violet for 15 min, and the cells inside the chamber were wiped off. After washing off the excess dye, the cells were photographed and counted with a microscope (Leica DM6B, Germany).

Apoptosis assay

Apoptosis was detected with the FITC Annexin V Apoptosis Detection Kit I (BD Biosciences, USA). Cells transfected for 48 h were collected and made into single cell suspensions. After adding Annexin V-FITC, incubate at room temperature for 15 min in the dark. PI was added 5 min before the test, and the flow cytometer CytoFlex (Beckman Coulter, USA) was used for detection.

Western blotting

Total cellular protein was extracted with RIPA lysate containing 1%

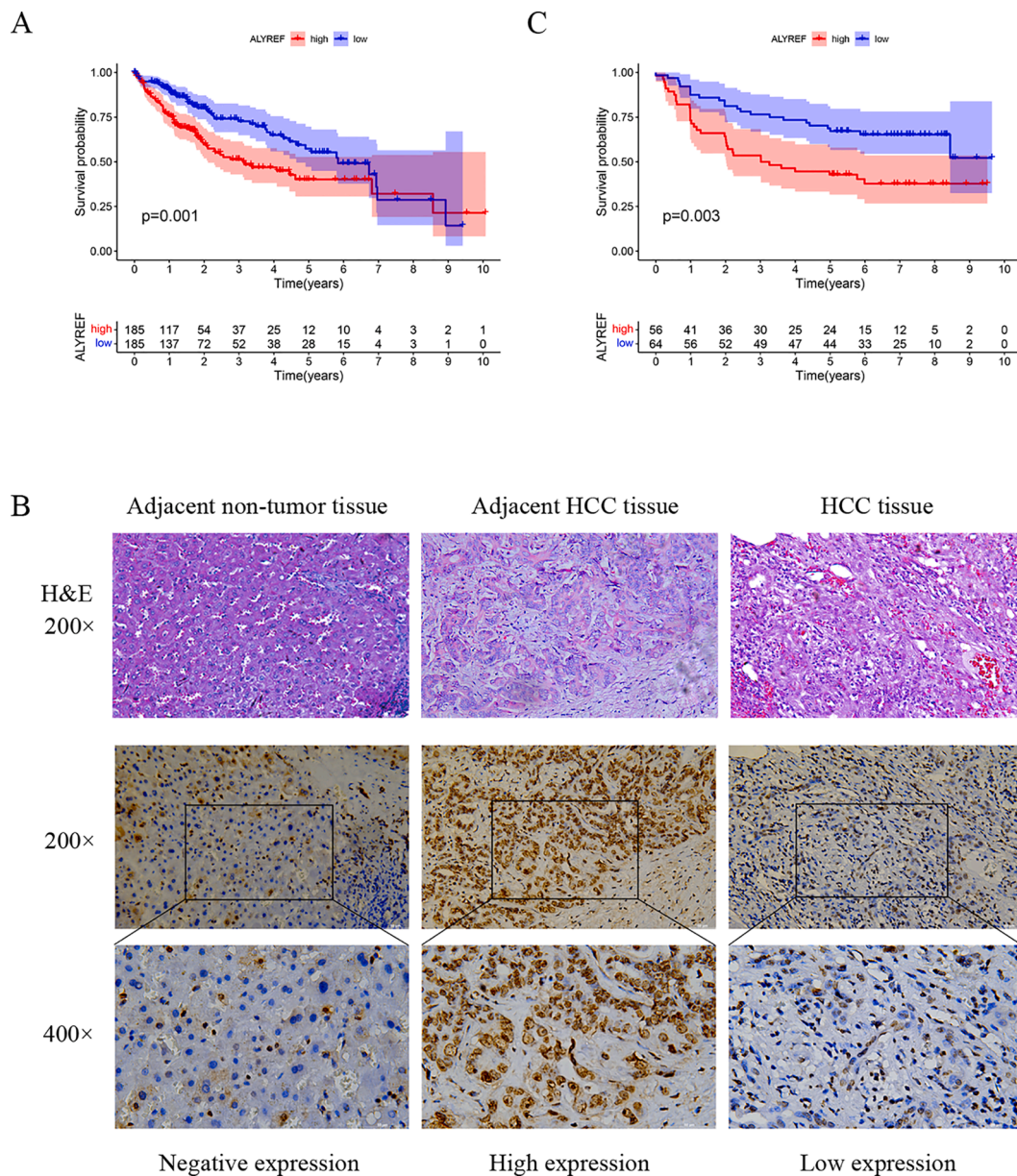


Fig. 2. *ALYREF* expression is upregulated in HCC and is associated with poor prognosis. (A) Survival analysis of *ALYREF* expression in the LIHC dataset. (B) Immunohistochemical staining images of *ALYREF* in tissue specimens. (C) Survival Analysis of *ALYREF* in 120 Hepatectomy Specimens.

protease inhibitor and quantified by BCA method. SDS-PAGE electrophoresis was used to transfer an equivalent amount of protein samples to PVDF membranes. After incubation with primary antibody (anti-*ALYREF*: abcam; anti-GAPDH: BBI life sciences) at 4 °C for overnight, incubate in secondary antibody for one hour at room temperature. Enhanced Chemiluminescence Kit (ECL) was used for the imaging with a chemiluminescence imaging system.

Immune cell infiltration

The effect of *ALYREF* on the abundance of infiltrating immune cell subsets in HCC, including macrophages, dendritic cells, neutrophils, CD4+ T cells, B cells and CD8+ T cells was evaluated by TIMER (<https://cistrome.shinyapps.io/timer/>) [14]. Since tumor purity can interfere with immune gene expression analysis, the results were corrected for it [15].

Immunomodulators and related genes

TISIDB (<http://cis.hku.hk/TISIDB/>) is a website where tumors and immune systems interact. Tumor-infiltrating lymphocytes (TILs) and immunomodulators associated with *ALYREF* were queried by TISIDB. These immunomodulatory genes were imported into cBioPortal (www.cbioportal.org) to further acquire the top 50 co-expressed genes. Related genes were submitted to GO annotation and KEGG enrichment analysis.

Survival analysis

The LIHC dataset was divided randomly and equally into a training set and a testing set. In the training set, univariate and multivariate Cox regression analysis was performed on *ALYREF*-related immune genes to construct prognostic markers. The risk score was calculated based on prognosis-related immune genes: Risk score = $\beta_1 \times x_1 + \beta_2 \times x_2 + \dots + \beta_{ixi}$. The expression of each prognosis-related gene in the tissue is represented by x_i , and β_i represents the risk factor of the prognostic gene

Table 3
Univariate and multivariate survival analysis of HCC patients in the LIHC database.

Parameter	Univariate analysis			Multivariate analysis		
	HR	95%CI	P	HR	95%CI	P
Age	0.993	0.615-1.601	0.976	1.137	0.684-1.889	0.621
Gender	0.780	0.487-1.249	0.301	0.927	0.560-1.534	0.769
Grade	1.017	0.746-1.387	0.914	1.010	0.726-1.404	0.954
Stage	1.865	1.456-2.388	8.07E-07	0.913	0.341-2.447	0.856
T	1.804	1.434-2.270	4.73E-07	1.889	0.774-4.610	0.163
M	3.850	1.207-12.281	0.023	1.281	0.337-4.870	0.717
N	2.022	0.494-8.276	0.328	2.176	0.381-12.411	0.382
ALYREF	1.021	1.011-1.031	1.56E-05	1.020	1.010-1.031	<0.001

calculated by Cox analysis. The relationship between risk score and overall survival was investigated via Kaplan-Meier survival analysis. The risk scores were evaluated via a time-dependent receiver operating characteristic (ROC) curve. A stepwise Cox analysis was used to identify independent prognostic factors. Internal validation is conducted with the testing set.

Constructing a nomogram

Nomograms are often applied to evaluate the prognosis of cancer patients because they can be personalized to assess the probability of a clinical event (e.g., recurrence, death), and the effect is mostly better than the TNM staging system [16]. Risk scores and patient clinical parameters were analyzed, and the 'rms' package of the R program was used to create nomograms. The deviation between predicted and actual probability is visualized by a calibration curve.

Statistical analysis

The statistics and graphing of the results were implemented by SPSS (version 22.0), GraphPad Prism (version 8), R software (version 4.0.4) and the aforementioned network tools. The R packages 'survival' and 'survival ROC' were used to plot the Kaplan-Meier survival curve and the time-dependent ROC curve, respectively. Spearman correlation analysis was used to determine relevant immune genes. Statistical significance was defined as a P value < 0.05.

Result

Upregulation of ALYREF in HCC and with poor prognosis

Bioinformatics analysis of the LIHC dataset showed that ALYREF expression was upregulated in HCC compared with paracancerous tissues (Fig. 1A,B). And the expression of ALYREF was related to tumor pathological grade, AJCC stage and T stage, but not to age, gender, M

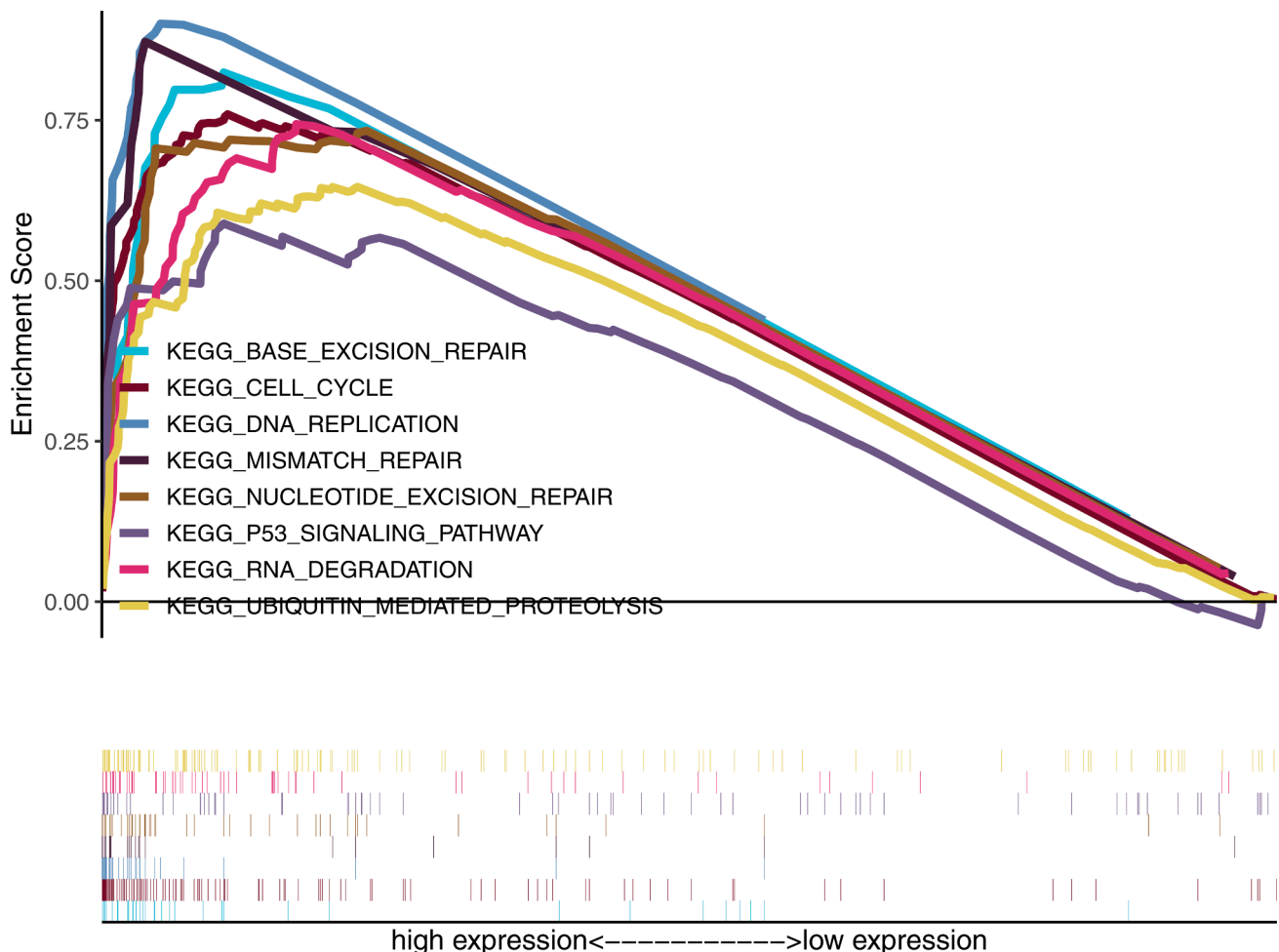


Fig. 3. Representative signaling pathways for ALYREF single gene GSEA analysis.

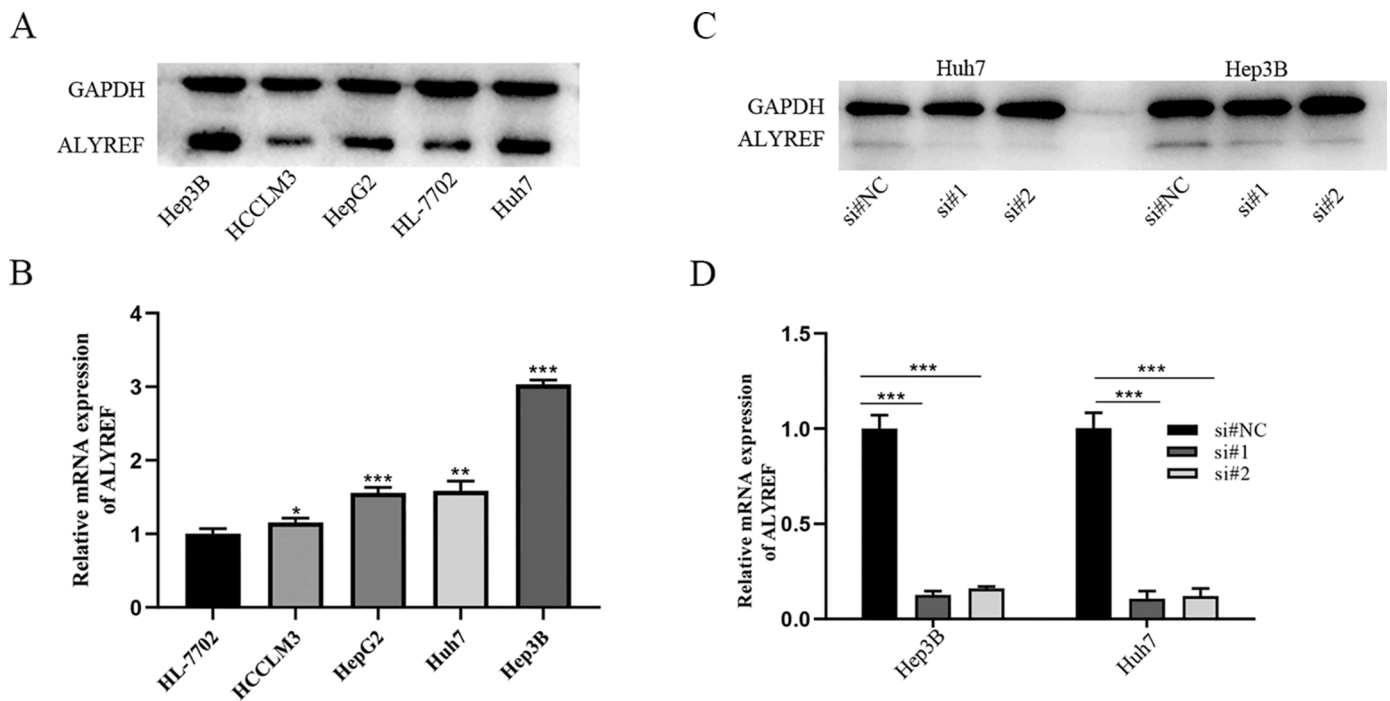


Fig. 4. *ALYREF* expression in HCC cell lines, and *ALYREF* knockdown efficiency. (A,B) Protein and mRNA expression levels of *ALYREF* in HL-7702 and HCC cell lines. (C,D) Expression of *ALYREF* in transfected Hep3B and Huh7 cells. Full-length blots are presented in Supplementary Fig. 2.

stage and N stage (Fig. 1C–I). *ALYREF* is expressed at higher levels in tissues with higher pathological grades (grade 3 and 4 compared to grade 1 and 2, respectively, Fig. 1E). Compared with AJCC stage I, higher expression of *ALYREF* was present in stages II and III (Fig. 1F). T staging results were similar (T2 vs T1, T3 vs T1, Fig. 1G). Survival analysis showed that patients in the higher *ALYREF* expression group had a worse prognosis (Fig. 2A). Meanwhile, stepwise regression analysis showed that *ALYREF* was an independent prognostic risk factor for HCC patients (Table 3). The GSEA results are shown in Fig. 3, and these pathways are mostly associated with cell growth.

Immunohistochemical staining showed that *ALYREF* protein levels were higher in tumor tissues compared with paracancerous ones (Fig. 2B). Representative data for the three staining intensities are presented in Supplementary Fig. 1. Moreover, Kaplan-Meier survival analysis also revealed that the patients with high *ALYREF* expression had a poor prognosis (Fig. 2C). Univariate and multivariate cox regression analysis of 120 surgical cases further indicated that *ALYREF* was an independent prognostic risk factor for HCC (Supplementary Table 1). The correlation analysis between *ALYREF* expression and other clinical indicators showed that *ALYREF* expression was connected to tumor pathological grade, AJCC stage, AFP expression level, vascular invasion, and tumor size (Table 1).

Correlation between *ALYREF* and biological behavior of HCC cell lines

The mRNA and protein expression of *ALYREF* in normal hepatocyte line HL-7702 and HCC cell lines (HCCLM3, Huh7, HepG2, and Hep3B) were detected by RT-qPCR and Western Blot (Fig. 4A,B). Based on the expression levels of *ALYREF* in HCC cell lines, Hep3B and Huh7 cells with higher expression levels were selected and transfected with specific siRNA to knock down *ALYREF* for further study. RT-qPCR and Western Blot revealed that si#1 and si#2 could effectively inhibit *ALYREF* expression compared with si#NC (Fig. 4C,D).

CCK-8, colony formation, scratch healing, and transwell invasion assays were used to study the effects of *ALYREF* on the proliferation, migration, and invasion of Hep3B and Huh7 cells. CCK-8 assay showed that *ALYREF*-si#1 and *ALYREF*-si#2 reduced the proliferation rate of

cells (Fig. 5A,B). Moreover, cells formed fewer colonies after *ALYREF* knockdown, further suggesting that *ALYREF* affects cell proliferation. (Fig. 5C,D). At 24 h after scratching, cells with knockdown of *ALYREF* had slower scratch healing and weaker migration capacity than si#NC, according to scratch healing assay data. (Fig. 5E,F). Invasiveness assay indicated that the number of cell invasion was dramatically reduced after knocking down *ALYREF* compared to si#NC (Fig. 5G,H). In addition, the detection of the effect of *ALYREF* on apoptosis by flow cytometry showed that knockdown of *ALYREF* promoted apoptosis. (Fig. 5I,J).

ALYREF and immune correlates

Since the abundance and activity of TILs can affect the survival time of patients with various tumors [17,18], we evaluated the correlation of *ALYREF* with TILs by TIMER and TISIDB. In TIMER, *ALYREF* was found to be positively linked with the level of immune cell subset infiltration. (Fig. 6A) and correlated with the abundance of multiple TILs in TISIDB (Fig. 6B). And in the TISIDB data portal, we found that *ALYREF* was associated with some immune modulator genes (Fig. 6B). These results suggest that alterations in *ALYREF* expression can affect the immunophenotype of HCC and influence patient prognosis.

Immune prognostic models and predictive value

To explore whether *ALYREF*-related immune genes can be translated into prognostic indicators for HCC patients, we selected 20 immunostimulators and 9 Immunoinhibitors associated with *ALYREF* and uploaded them to cBioPortal to get the top 50 genes that are closely connected. GO and KEGG results indicated that these genes were implicated in multiple immune functions and immune regulatory pathways (Fig. 6C,D). Stepwise regression analysis was applied on these genes in the LIHC training set, and 4 immune genes affecting prognosis were screened out, thus constituting a prognosis model for HCC (Fig. 7A,B) and to calculate the risk score. Overall survival in the high-risk group was shorter than in the low-risk group, according to the Kaplan Meier survival curve. (Fig. 7C). The great dependability was revealed by the time-dependent ROC curve.

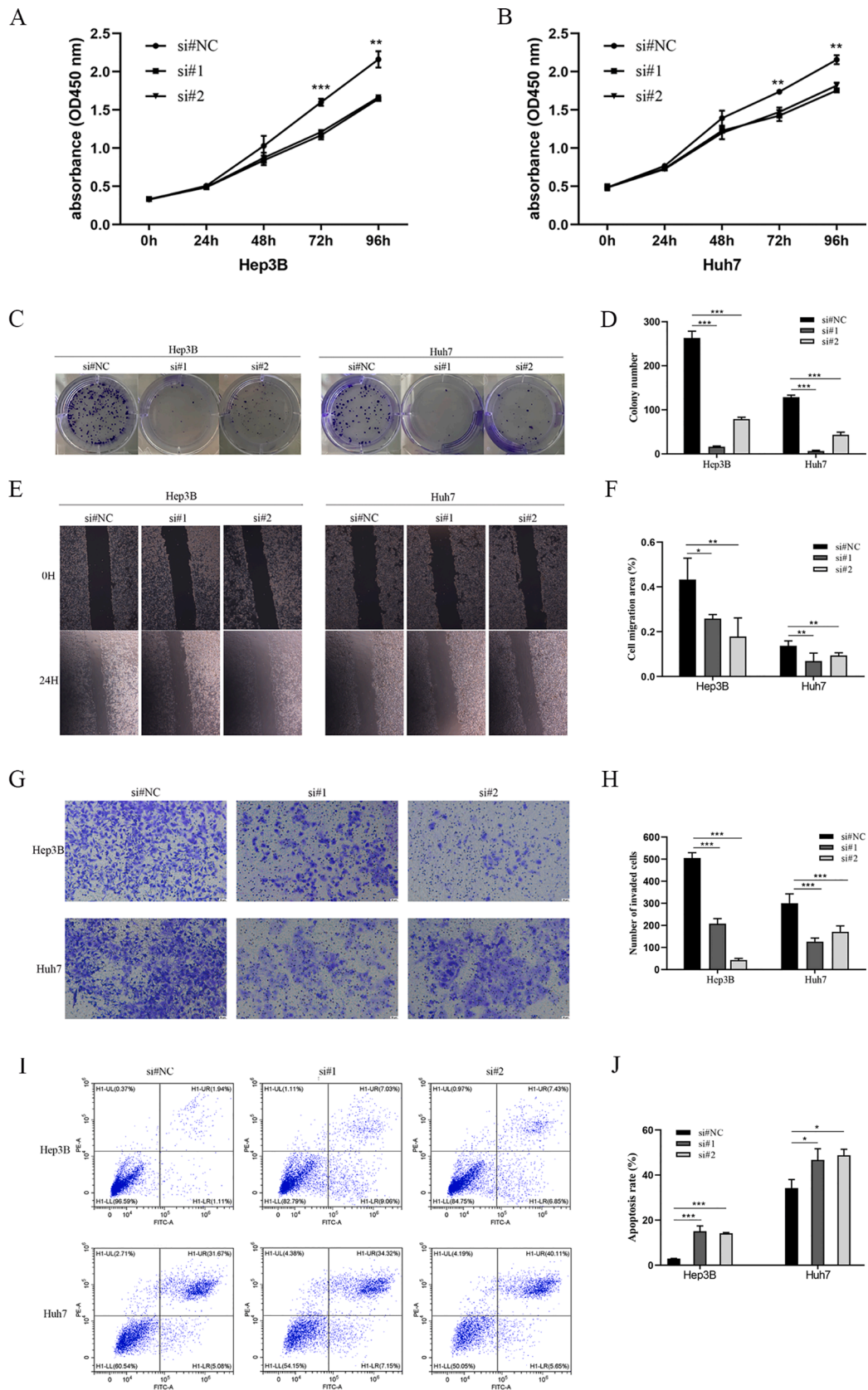


Fig. 5. Effect of *ALYREF* on proliferation, migration, invasion and apoptosis of HCC cells. (A,B) Proliferative capacity of Hep3B and Huh7 cells after transfection. (C, D) Colony-forming ability of Hep3B and Huh7 cells after transfection. (E,F) Migration ability of Hep3B and Huh7 cells after transfection. (G,H) invasive ability of Hep3B and Huh7 cells after transfection. (I,J) Apoptosis rates of Hep3B and Huh7 cells after transfection. * $P < 0.05$, ** $P < 0.01$, *** $P < 0.001$.

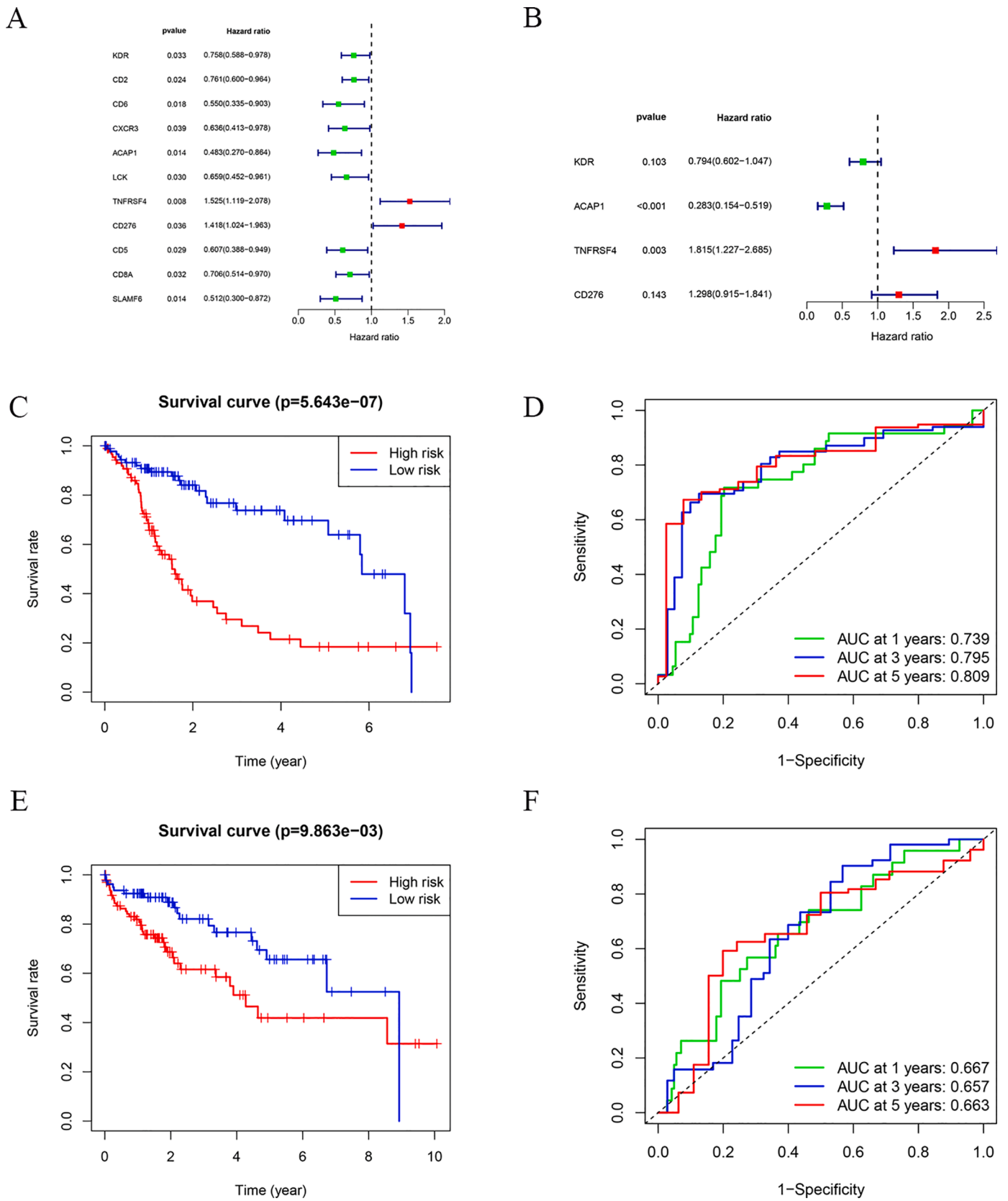


Fig. 7. Develop prognostic gene signatures based on 79 *ALYREF*-related immune genes. (A) Univariate Cox regression analysis. (B) Multivariate Cox regression analysis. (C) Survival analysis of the LIHC training set risk score. (D) Time-dependent ROC curves for the prognostic model of the LIHC training set. (E) Survival analysis of the LIHC testing set risk scores. (F) Time-dependent ROC curves for the prognostic model of the LIHC testing set.

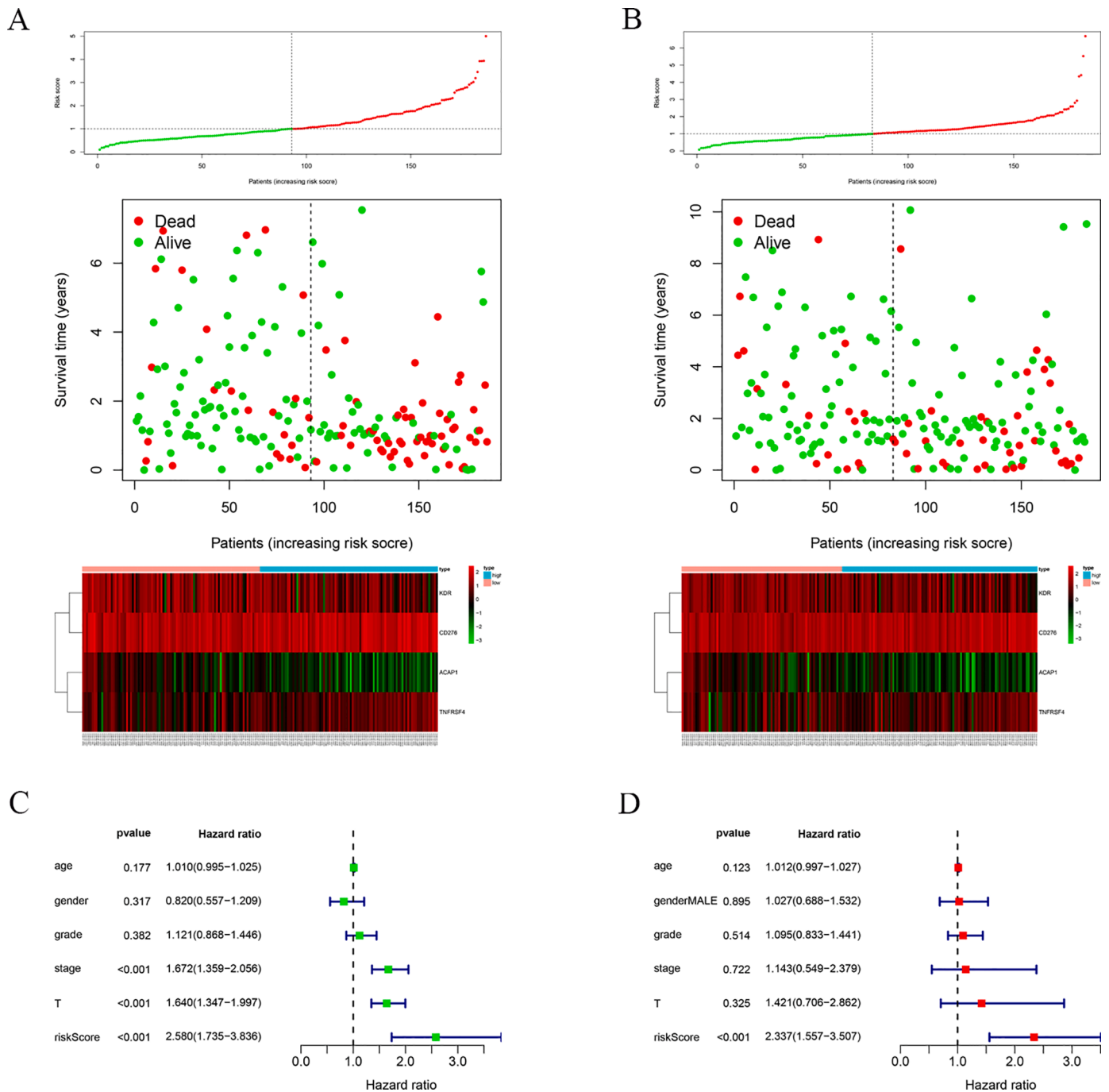


Fig. 8. Prognostic value of risk scores. (A,B) Plots of risk score distribution, survival status, and gene expression patterns of HCC patients in LIHC training and testing sets. (C,D) Univariate and multivariate Cox regression analyzes of the relationship between risk score and overall survival.

immune cells in the tumor microenvironment, which in turn affects tumor progression.

Several studies have shown that immune-related genes can be utilized as markers to evaluate the prognosis and responsiveness to immunotherapy in tumor patients [30-32]. Therefore, we developed a prognostic model consisting of four immune-related genes (KDR, ACAP1, TNFRSF4 and CD276) based on *ALYREF*-related immune genes. KDR has been shown to predict the prognosis of HCC patients and is a target for HCC treatment [33,34]. Xie et al [35] have stated that TNFRSF4 is strongly associated with the immune microenvironment of HCC and contributes to poor prognosis. CD276 is a potential target for HCC immunotherapy and can be utilized as a predictor of survival in HCC patients [36-38]. It indicated that the prognostic model we

constructed provided potential therapeutic targets and prognostic assessment indicators for immunotherapy of HCC.

Conclusions

Our study preliminarily showed that *ALYREF* can serve as a prognostic marker for HCC and has an important biological function in the progression of HCC. The resulting immune prognostic markers allow for the assessment of patient survival and provide targets for immunotherapy. These provide further insights into the role of *ALYREF* in HCC progression and immunotherapy. In conclusion, *ALYREF* plays a crucial role in HCC immunity, affects patient prognosis, and may be a viable immunotherapy target.

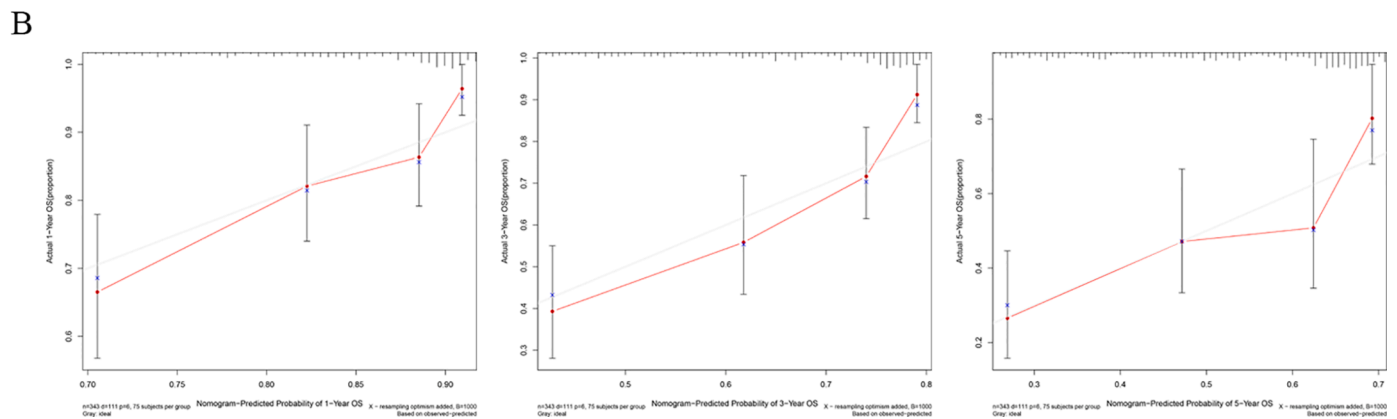
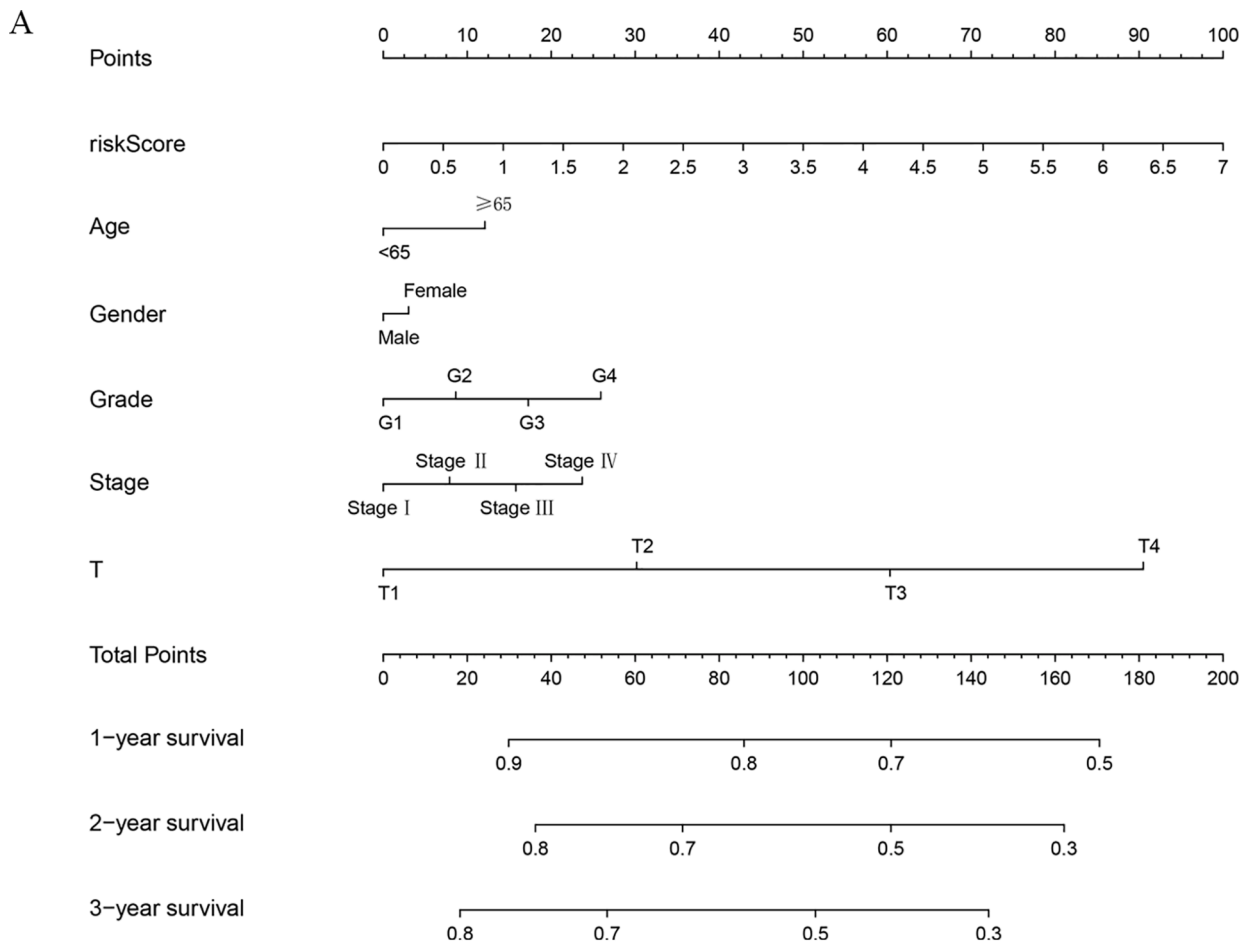


Fig. 9. Risk scores were incorporated to construct a prognostic nomogram. (A) Nomogram predicting 1-, 3-, and 5-year survival probabilities of HCC patients. (B) Calibration curves of nomogram-predicted 1-, 3-, and 5-year survival of HCC patients.

CRediT authorship contribution statement

Zhen-Zhen Wang: Conceptualization, Methodology, Validation, Formal analysis, Writing – original draft. **Tao Meng:** Software, Validation, Formal analysis. **Ming-Ya Yang:** Software, Validation, Formal analysis. **Wei Wang:** Investigation, Resources. **Yan Zhang:** Investigation, Resources. **Yu Liu:** Investigation, Resources. **An-Qi Han:** Investigation, Resources. **Jin Wu:** Investigation, Resources. **Hui-xiao Wang:** Supervision. **Bo Qian:** Supervision. **Li-Xin Zhu:** Conceptualization, Writing – review & editing, Funding acquisition.

Declaration of Competing Interest

The authors declare that they have no known competing financial interests or personal relationships that could have appeared to influence the work reported in this paper

Funding

The work is supported by the National Natural Science Foundation of China (grant numbers: 52072005 and 51872279).

Data Availability Statement

The public datasets used in this study can be found here: The Cancer Genome Atlas (<https://portal.gdc.cancer.gov/>).

Ethics approval and consent to participate

Approved by the Medical Ethics Committee of the First Affiliated Hospital of Anhui Medical University.

Consent for publication

Not applicable

Supplementary materials

Supplementary material associated with this article can be found, in the online version, at doi:10.1016/j.tranon.2022.101441.

References

- [1] H. Sung, J. Ferlay, R.L. Siegel, M. Laversanne, I. Soerjomataram, A. Jemal, et al., Global cancer statistics 2020: GLOBOCAN estimates of incidence and mortality worldwide for 36 cancers in 185 countries, *CA Cancer J. Clin.* 71 (3) (2021) 209–249.
- [2] J.M. Llovet, R.K. Kelley, A. Villanueva, A.G. Singal, E. Pikarsky, S. Roayaie, et al., Hepatocellular carcinoma, *Nat. Rev. Dis. Primers* 7 (1) (2021) 6.
- [3] Z.J. Brown, T.F. Greten, B. Heinrich, Adjuvant treatment of hepatocellular carcinoma: prospect of immunotherapy, *Hepatology* 70 (4) (2019) 1437–1442.
- [4] C. Kole, N. Charalampakis, S. Tsakatikas, M. Vailas, D. Moris, E. Gkotsis, et al., Immunotherapy for hepatocellular carcinoma: a 2021 update, *Cancers* 12 (10) (2020) (Basel).
- [5] Y.H. Lee, D. Tai, C. Yip, S.P. Choo, V. Chew, Combinational immunotherapy for hepatocellular carcinoma: radiotherapy, immune checkpoint blockade and beyond, *Front. Immunol.* 11 (2020), 568759.
- [6] J. Fan, K. Wang, X. Du, J. Wang, S. Chen, Y. Wang, et al., *ALYREF* links 3'-end processing to nuclear export of non-polyadenylated mRNAs, *EMBO J.* 38 (9) (2019).
- [7] M. Munschauer, C.T. Nguyen, K. Sirokman, C.R. Hartigan, L. Hogstrom, J. M. Engreitz, et al., The NORAD lncRNA assembles a topoisomerase complex critical for genome stability, *Nature* 561 (7721) (2018) 132–136.
- [8] J.Z. Wang, W. Zhu, J. Han, X. Yang, R. Zhou, H.C. Lu, et al., The role of the HIF-1 α /*ALYREF*/*PKM2* axis in glycolysis and tumorigenesis of bladder cancer, *Cancer Commun.* 41 (7) (2021) 560–575 (Lond).
- [9] Z. Nagy, J.A. Seneviratne, M. Kanikevich, W. Chang, C. Mayoh, P. Venkat, et al., An *ALYREF*-MYC coactivator complex drives neuroblastoma tumorigenesis through effects on USP3 and MYC stability, *Nat. Commun.* 12 (1) (2021) 1881.
- [10] M. Xue, Q. Shi, L. Zheng, Q. Li, L. Yang, Y. Zhang, Gene signatures of m5C regulators may predict prognoses of patients with head and neck squamous cell carcinoma, *Am. J. Transl. Res.* 12 (10) (2020) 6841–6852.
- [11] Y. Saito, A. Kasamatsu, A. Yamamoto, T. Shimizu, H. Yokoe, Y. Sakamoto, et al., *ALY* as a potential contributor to metastasis in human oral squamous cell carcinoma, *J. Cancer Res. Clin. Oncol.* 139 (4) (2013) 585–594.
- [12] J. Wang, Y. Li, B. Xu, J. Dong, H. Zhao, D. Zhao, et al., *ALYREF* drives cancer cell proliferation through an *ALYREF*-MYC positive feedback loop in glioblastoma, *Onco Targets Ther.* 14 (2021) 145–155.
- [13] C. Xue, Y. Zhao, G. Li, L. Li, Multi-omic analyses of the m(5)c regulator *ALYREF* reveal its essential roles in hepatocellular carcinoma, *Front. Oncol.* 11 (2021), 633415.
- [14] T. Li, J. Fan, B. Wang, N. Traugh, Q. Chen, J.S. Liu, et al., TIMER: a web server for comprehensive analysis of tumor-infiltrating immune cells, *Cancer Res.* 77 (21) (2017) e108–e110.
- [15] J.K. Rhee, Y.C. Jung, K.R. Kim, J. Yoo, J. Kim, Y.J. Lee, et al., Impact of tumor purity on immune gene expression and clustering analyses across multiple cancer types, *Cancer Immunol. Res.* 6 (1) (2018) 87–97.
- [16] A. Iasonos, G.V. Raj, K.S. Panageas, How to build and interpret a nomogram for cancer prognosis, *J. Clin. Oncol.* 26 (8) (2008) 1364–1370.
- [17] S.T. Pajjens, A. Vledder, M. de Bruyn, H.W. Nijman, Tumor-infiltrating lymphocytes in the immunotherapy era, *Cell Mol. Immunol.* 18 (4) (2021) 842–859.
- [18] L. Li, L. Shen, J. Ma, Q. Zhou, M. Li, H. Wu, et al., Evaluating distribution and prognostic value of new tumor-infiltrating lymphocytes in HCC based on a scRNA-seq study with CIBERSORTx, *Front Med* 7 (2020) 451 (Lausanne).
- [19] W. Wang, C. Wei, Advances in the early diagnosis of hepatocellular carcinoma, *Genes Dis.* 7 (3) (2020) 308–319.
- [20] J. Prieto, I. Melero, B. Sangro, Immunological landscape and immunotherapy of hepatocellular carcinoma, *Nat. Rev. Gastroenterol. Hepatol.* 12 (12) (2015) 681–700.
- [21] M. Inarrairaegui, I. Melero, B. Sangro, Immunotherapy of hepatocellular carcinoma: facts and hopes, *Clin. Cancer Res.* 24 (7) (2018) 1518–1524.
- [22] M. Macheret, T.D. Halazonetis, DNA replication stress as a hallmark of cancer, *Ann. Rev. Pathol.* 10 (2015) 425–448.
- [23] P.R. Clarke, L.A. Allan, Cell-cycle control in the face of damage—a matter of life or death, *Trends Cell Biol.* 19 (3) (2009) 89–98.
- [24] Y. Fu, S. Liu, S. Zeng, H. Shen, From bench to bed: the tumor immune microenvironment and current immunotherapeutic strategies for hepatocellular carcinoma, *J. Exp. Clin. Cancer Res.* 38 (1) (2019) 396.
- [25] F. Heymann, F. Tacke, Immunology in the liver—from homeostasis to disease, *Nat. Rev. Gastroenterol. Hepatol.* 13 (2) (2016) 88–110.
- [26] X. Liu, S. Wu, Y. Yang, M. Zhao, G. Zhu, Z. Hou, The prognostic landscape of tumor-infiltrating immune cell and immunomodulators in lung cancer, *Biomed. Pharmacother.* 95 (2017) 55–61.
- [27] Q.Y. Zhong, E.X. Fan, G.Y. Feng, Q.Y. Chen, X.X. Gou, G.J. Yue, et al., A gene expression-based study on immune cell subtypes and glioma prognosis, *BMC Cancer* 19 (1) (2019) 1116.
- [28] B. Lin, L. Du, H. Li, X. Zhu, L. Cui, X. Li, Tumor-infiltrating lymphocytes: warriors fight against tumors powerfully, *Biomed. Pharmacother.* 132 (2020), 110873.
- [29] N. Rohr-Udilova, F. Klingmuller, R. Schulte-Hermann, J. Stift, M. Herac, M. Salzmann, et al., Deviations of the immune cell landscape between healthy liver and hepatocellular carcinoma, *Sci. Rep.* 8 (1) (2018) 6220.
- [30] S. Wang, Y. Xiong, Q. Zhang, D. Su, C. Yu, Y. Cao, et al., Clinical significance and immunogenomic landscape analyses of the immune cell signature based prognostic model for patients with breast cancer, *Brief Bioinform* 22 (4) (2021).
- [31] S. Shen, G. Wang, R. Zhang, Y. Zhao, H. Yu, Y. Wei, et al., Development and validation of an immune gene-set based prognostic signature in ovarian cancer, *EBioMedicine* 40 (2019) 318–326.
- [32] W. Chen, M. Ou, D. Tang, Y. Dai, W. Du, Identification and validation of immune-related gene prognostic signature for hepatocellular carcinoma, *J. Immunol. Res.* 2020 (2020), 5494858.
- [33] R. Shang, X. Song, P. Wang, Y. Zhou, X. Lu, J. Wang, et al., Cabozantinib-based combination therapy for the treatment of hepatocellular carcinoma, *Gut* 70 (9) (2021) 1746–1757.
- [34] K. Shigeta, M. Datta, T. Hato, S. Kitahara, I.X. Chen, A. Matsui, et al., Dual programmed death receptor-1 and vascular endothelial growth factor receptor-2 blockade promotes vascular normalization and enhances antitumor immune responses in hepatocellular carcinoma, *Hepatology* 71 (4) (2020) 1247–1261.
- [35] K. Xie, L. Xu, H. Wu, H. Liao, L. Luo, M. Liao, et al., OX40 expression in hepatocellular carcinoma is associated with a distinct immune microenvironment, specific mutation signature, and poor prognosis, *Oncoimmunology* 7 (4) (2018), e1404214.
- [36] Y. Xu, Z. Zhang, D. Xu, X. Yang, L. Zhou, Y. Zhu, Identification and integrative analysis of *ACL*Y and related gene panels associated with immune microenvironment reveal prognostic significance in hepatocellular carcinoma, *Cancer Cell Int.* 21 (1) (2021) 409.
- [37] T.W. Sun, Q. Gao, S.J. Qiu, J. Zhou, X.Y. Wang, Y. Yi, et al., B7-H3 is expressed in human hepatocellular carcinoma and is associated with tumor aggressiveness and postoperative recurrence, *Cancer Immunol. Immunother.* 61 (11) (2012) 2171–2182.
- [38] L. Luo, H. Qiao, F. Meng, X. Dong, B. Zhou, H. Jiang, et al., Arsenic trioxide synergizes with B7H3-mediated immunotherapy to eradicate hepatocellular carcinomas, *Int. J. Cancer* 118 (7) (2006) 1823–1830.